IEEE Access
Multidisciplinary | Rapid Review | Open Access Journal

Received 13 March 2023, accepted 2 April 2023, date of publication 5 April 2023, date of current version 10 April 2023.

Digital Object Identifier 10.1109/ACCESS.2023.3264530

RESEARCH ARTICLE

Design and Implementation of an Efficient Wake-Up Synchronization Scheme Based on History in a 5G Software Modem

SUBIN JEONG, (Student Member, IEEE), AND JUYEOP KIM, (Member, IEEE)
Department of Electrical Engineering, Sookmyung Women's University, Seoul 04310, South Korea

Corresponding author: Juyeop Kim (jykim@sookmyung.ac.kr)

This work was supported in part by the Institute for Information and Communications Technology Promotion (IITP) Grant funded by the Korean Government (MSIP; 2018-0-00726, "Development of Software-Defined Cell/Beam Search Technology for Beyond-5G Systems"); and in part by the Basic Science Research Program through the National Research Foundation of Korea (NRF) funded by the Ministry of Education under Grant 2021R1F1A1061951.

ABSTRACT 5G adopts Discontinuous Reception (DRX) technology, which enables the User Equipment (UE) to repeat sleep and wake-up cycles for power-saving. To minimize power consumption, the UE needs to re-synchronize to a downlink signal transmitted from a serving gNodeB (gNB) for each DRX occasion. To have a synchronization technique suitable to DRX occasions, we design and implement a history-based synchronization scheme that can effectively manage the window of synchronization signal detection. The proposed scheme primarily considers the statistics of previously detected timing offsets when configuring the window of synchronization. The history information is formatted appropriately for calculating the drift of the timing offset on each DRX occasion. The proposed scheme also monitors multi-path environments and extends the detection window to the timing offset of the second path based on the probabilistic model. To demonstrate its performance, the proposed scheme is implemented on a software modem so that it can be processed in real-time. The experimental results demonstrate that the proposed scheme can reduce computational complexity and achieve more precise synchronization in a low Signal to Noise Ratio (SNR) regime.

INDEX TERMS 5G, synchronization, cell search, discontinuous reception, primary synchronization signal, multi-path fading, software modem.

I. INTRODUCTION

A mobile communications system has been recently driven to 5G by the 3rd Generation Partnership Project (3GPP). Although this new system heads toward advanced features, it inherits the conventional feature of Discontinuous Reception (DRX) [1]. The DRX specifies the occasions of downlink transmissions to guarantee that User Equipments (UEs) conduct power-saving operations between the occasions. As the lifetime of every UE relies on its battery, the DRX has been vital to mobile communications since earlier generations. Moreover, the recent mobile terminals are required to execute various applications and complicated computations, so a 5G UE critically needs to conduct the DRX for prolonging its lifetime at a reasonable level.

Numerous works of research have recognized the significance of DRX and addressed related power consumption issues. Optimized DRX parameters are applied to Long Term Evolution (LTE) to enhance power saving [2]. The efficient DRX cycle schemes, such as Enhanced Paging Monitoring (EPM) and Extended Discontinuous Reception (eDRX), aim to minimize radio resource overhead in the 5G [3], [4], [5]. In addition, a beam-aware DRX scheme [6] and Partitioned UE ID-based Directional Paging (PIDP) [7] are applied to alleviate the computational burden of beam search in the 5G.

The associate editor coordinating the review of this manuscript and approving it for publication was Nurul I. Sarkar.

One practical issue for the UEs in DRX mode is to recover synchronization before the next downlink reception. For power-saving purposes, the UE generally turns its receiver hardware off until the next DRX occasion, so the downlink synchronization is not maintained continuously. Consequently, the UE should resynchronize with the downlink signal during a wake-up operation. Unfortunately, a general synchronization approach is not appropriate in this instance since it requires a considerable amount of time compared to the downlink reception time at the DRX occasion. The general synchronization procedure consumes more power than the downlink reception and is undesirable for the wake-up operation from a power-saving standpoint.

Hence, the wake-up operation needs to have a differentiated method to accomplish synchronization efficiently. A 5G UE essentially estimates symbol timing, carrier frequency offset (CFO), and Physical Cell ID (PCI) through synchronization. Among these factors, estimating the symbol timing occupies a significant portion of the total synchronization time. This is because the UE initially estimates the symbol timing by detecting Primary Synchronization Signal (PSS) blindly without any prior information [8]. Therefore, the UE in the DRX mode should focus on reducing the computational complexity of the PSS detection to shorten the wake-up operation.

Prior research has suggested various schemes to improve the complexity of the PSS detection. Integer carrier frequency offset and the PSS sequence are jointly detected via two sequential detection tasks utilizing the auto-correlation property of the PSS sequence [8]. Using the central-symmetric properties of the LTE and 5G synchronization signals, some research works propose to reduce the number of multiplications for calculating correlation [9], [10], [11]. In these works, the amount of multiplications is reduced based on K-means clustering [10] and two improved PSS detectors are presented for operating correlation of the half of the sequence [11]. On the other hand, some research works improve the detection performance by enhancing robustness to frequency offset in a low Signal to Noise Ratio (SNR) regime [12], [13]. However, none of these research works are applied to the DRX situation in which the UE periodically synchronizes to the downlink signal.

One effective approach to conducting the PSS detection at DRX occasions is to utilize detection history. This approach is based on the assumption that the current synchronization result is somehow associated with the previous ones. In DRX mode, the UE periodically conducts the PSS detection at each DRX occasion so that it can accumulate the history of detected symbol timing. If the UE can configure a detection window with a specific interval in which the PSS is likely to exist through the history, it can focus on detecting the PSS in the window at the next DRX occasion. The PSS detection time is linearly proportional to the detection interval, so having a shorter interval will reduce the power consumption of the wake-up operation.

There are two challenging issues while configuring the detection window in the DRX mode. The UE needs to configure the detection window by considering various time-varying factors of a wireless channel. The symbol timing experiences drifting since the sampling clock frequency differs at the transmitter and receiver sides [14], [15]. This drift phenomenon is considered a kind of sampling error. Hence, observing how the previous symbol timing drifts is significant in configuring the detection window. The detection window also needs to be wide enough to cover the variance of the symbol timing drifts. In addition, the UE in a multi-path channel environment should detect and manage multiple symbol timings to achieve the suitable synchronization performance at a low SNR regime [16], [17], [18]. Accordingly, it is essential for the UE to adapt the detection window in real time based on the observation of symbol timing changes.

Several conventional research works handle the issue of the detection window configuration. A PSS detection scheme utilizes a windowing concept to consider power delay properties in a multi-path fading environment [19]. This scheme aims to enhance its detection accuracy by taking the average of correlation results within a window, whereas it does not consider reducing computational complexity. There are other timing synchronization strategies that estimate the time offset based on deep-learning (DL) [20], [21], [22]. Extreme Learning Machine (ELM) detects the residual elements of time and frequency offset through the training process to improve synchronization performance, whereas it has substantial computation delay and vulnerability to the rapid change of channel state information [20]. The scheme using a time auto-regression model is presented to reduce detection latency but does not consider the time-varying factors [21]. Finally, timing synchronization based one-dimensional convolutional neural network (1-D-CNN) and designing filter (i.e. window) size enhances timing accuracy by considering power delay profile (PDP) in Line Of Sight (LOS) scenarios with increased computational complexity [22]. A sliding differential mirror correlation exploits an accumulated result based on the symmetric property of the PSS in a time domain [23]. This correlation scheme can improve detection performance in a low SNR regime but does not resolve the complexity issue of PSS detection. Some schemes configure a suitable window size for detecting the PSS based on Cyclic Prefix (CP) [24], [25]. One of them detects the PSS in a frequency domain by initially estimating the coarse timing of the OFDM symbol boundary with CPs [24]. This approach can contribute to reducing the complexity of PSS detection. However, it is disadvantageous if a gNB does not transmit signals continuously and no OFDM symbol is present for a given interval. The other scheme detects the length of a CP in the presence of timing and frequency offset uncertainty, but does not provide timing offset [25].

In this paper, we design and implement an advanced synchronization scheme for the wake-up procedure of a UE in

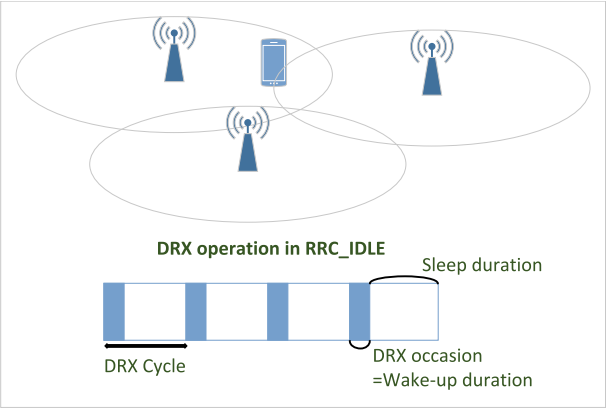

FIGURE 1. The system model of the UE in RRC_IDLE state.

DRX mode. Based on information about the previous PSS detection, the UE adaptively configures a detection window to enhance its performance and efficiency simultaneously and points to future research. For practical verification, we implement the proposed scheme based on the SoftWare (SW) modem, in which the algorithmic operations of the baseband signal processing are taken by software running on a general-purpose CPU. The remainder of this paper is structured as follows. Section II presents the overall system model of the proposed scheme. Section III explains how the proposed scheme derives and configures the detection window from history parameters. Section IV describes the experiments for evaluating the detection performance in laboratory and commercial environments. Finally, Section V concludes this paper.

II. SYSTEM MODEL

We assume that a 5G UE has camped on a serving cell and is in an RRC_IDLE state as shown in Fig. 1. The UE has accomplished a cell selection procedure, so it has synchronized to the downlink signal of the gNB and acquired system information of the cell [26]. After network registration, an end-to-end bearer is configured across the 5G network and the UE is prepared to receive terminating data via the bearer. The UE does not have an uplink channel and only receives a minimal downlink signal indicating its terminating data unless an uplink data traffic is generated. Instead of receiving the downlink signal for the whole duration, the UE conducts a power-saving operation and attempts to keep its hardware status off.

To keep the network connectivity of the UE, the 5G network should have a way to access the UE at any moment that terminating data arrives. Therefore, the UE in the RRC_IDLE state conducts DRX at various occasions predetermined with the 5G network [27]. For each camped UE, the 5G network initially indicates its terminating data by sending a paging message on a UE-specific DRX occasion. When the UE receives the paging message at its specific DRX occasion, it tries to transit its state to RRC_CONNECTED and to receive data continuously via a downlink channel. To see whether a paging message arrives or not, the UE should periodically monitor the Physical Downlink Control Channel (PDCCH) for each DRX occasion. This reveals that the UE needs to synchronize to the downlink signal and decode the PDCCH at the DRX occasions to sustain its network connectivity.

As the UE is not required to receive the downlink signal between the DRX occasions, the UE goes to *sleep* by turning its receiver hardware off until the next DRX occasion. The asleep UE wakes up by reactivating the receiver hardware before monitoring the PDCCH at the DRX occasion. The 5G network typically configures the periodicity of the DRX occasions at 320, 640, 1280, or 2560 ms [28], which is a long time in a synchronization aspect. Instead of keeping synchronized all the time, the UE accomplishes downlink synchronization just before the beginning of the DRX occasion. Meanwhile, the UE needs to conduct precise synchronization having the fine performance of the PDCCH monitoring. It is also important that the synchronization should be accomplished in short time so that the UE takes little time on the wake-up and minimizes its power-saving interval. Since the time interval of the PDCCH monitoring is less than a slot, synchronization before the PDCCH monitoring should take much shorter time than initial synchronization.

A. SYNCHRONIZATION SIGNAL BLOCKS

A synchronization procedure is conducted based on a Synchronization Signal Block (SSB) which is periodically broadcasted by the gNB. Unlike LTE, in which synchronization signals are transmitted once in a half-frame, the gNB sends several SSBs to enable the UE to distinguish multiple beams. The gNB transmits an SSB for each beam at a different moment, so an SSB burst which consists of several SSBs is periodically transmitted for each half-frame. The UE in the RRC_IDLE state selects one of the SSBs which corresponds to its best beam and synchronizes the downlink signal via the selected SSB for every DRX occasion. Fig. 2 illustrates an example of an SSB burst transmission pattern in the time domain. The SSB burst pattern depends on the numerology of the 5G system, and the indices of slots and OFDM symbols that contain the SSB can be given by the numerology [29].

As shown in Fig. 2, an SSB is composed of two synchronization signals and a channel, denoted by Primary Synchronization Signal (PSS) and Secondary Synchronization Signal (SSS), and Physical Broadcast Channel (PBCH). During a synchronization procedure, the UE acquires $N_{ID}^{(2)} \in \{0, 1, 2\}$ as well as timing and frequency offsets through PSS detection, and then $N_{ID}^{(1)} \in \{0, 1, \ldots, 335\}$ through SSS detection. After the PSS and SSS detection, the PCI, denoted by N_{ID}, is derived by combining $N_{ID}^{(1)}$ and $N_{ID}^{(2)}$ as follows,

$$N_{ID} = N_{ID}^{(2)} + 3N_{ID}^{(1)}. \tag{1}$$

The UE then decodes the PBCH to obtain system information and the index of the beam that provides the received SSB.

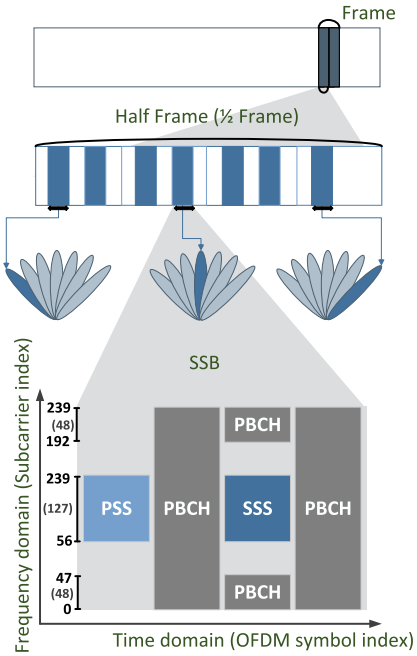

FIGURE 2. The architecture of an SSB.

As stated above, PSS detection is significant during the wake-up synchronization procedure. The symbol sequence of the PSS, denoted by d_{PSS}, corresponds to an m-sequence generated based on $N_{ID}^{(2)}$. It is mathematically described as follows [30],

$$d_{PSS,i}[n] = 1 - 2x[m] \tag{2}$$

$$m = (n + 43i) \bmod 127, \tag{3}$$

where $i = N_{ID}^{(2)}$. These PSS symbols are mapped from the 56-th to 182-nd subcarriers in the first OFDM symbol of the SSB, while the other subcarriers in the first OFDM symbol are padded with zero.

B. CHANNEL MODEL AND PSS DETECTION

We assume that the UE experiences Rayleigh multi-path fading and receives the SSB via M paths. Denoting $r[n]$ as received time-domain samples,

$$r[n] = \sum_{m=0}^{M-1} h_m s_i[n - \theta_m] + z[n], \tag{4}$$

where $s_i[n]$ is the transmitted time-domain samples of the SSB whose $N_{ID}^{(2)}$ is i, h_m and θ_m are channel gain and delay of the m-th path, respectively, and $z[n]$ is a zero-mean complex Gaussian Noise. h_m is the factor in terms of the fading channel and is a random variable with the following probability distribution,

$$P(h_m = x) = \frac{x \exp(\frac{-x^2}{2\sigma_m^2})}{\sigma_m^2}, \tag{5}$$

where σ_m is the scale parameter of the m-th path fading.

Under the above channel environment, the UE estimates the channel components h_m and θ_m in (4) via the PSS detection. θ_m is derived by calculating auto-correlation, denoted by $\rho_i[\theta]$ as follows,

$$\rho_i[\theta] = \sum_{k=0}^{N-1} r[\theta + k] p_i[k], \tag{6}$$

where N is the length of an OFDM symbol without CP and $p_i[n]$ is transmitted time-domain samples containing $d_{PSS,i}$. The UE can find out θ_m by observing the m-th peak position of $\rho_i[\theta]$. It estimates the timing offset and $N_{ID}^{(2)}$, denoted by $\hat{\theta}_{max}$ and $\hat{N}_{ID}^{(2)}$ respectively, as follows,

$$(\hat{N}_{ID}^{(2)}, \hat{\theta}_{max}) = \arg\max_{(i,\theta)} (\rho_i[\theta]) . \tag{7}$$

III. DESIGN OF HISTORY-BASED WAKE-UP SYNCHRONIZATION

The main idea of the proposed scheme lies in utilizing the previous history for synchronization to reduce computational complexity. If the UE can configure a detection window before calculating the auto-correlation, it can efficiently conduct a window search by processing the auto-correlation within the range of the detection window. In the RRC_IDLE state, the UE can use the information of the timing offset obtained from the previous DRX occasions for configuring the detection window at the current DRX occasion. Moreover, the UE repeats estimating and compensating CFO via synchronization. The UE only needs to handle residual CFO during the wake-up synchronization. However, the previous timing offset is not directly applicable after a DRX cycle due to various time-varying factors. Even as the influence of multi-path terms in (6) changes over time and may get more potent in a commercial environment [17], the fading factors need to be properly considered while configuring the detection window. Therefore, the proposed scheme adaptively manages the size of the detection window with a *margin*. This margin can be determined based on estimating the fading channel that the UE has previously experienced.

A. DEFINING A HISTORY DATABASE

The proposed scheme stores the information necessary for setting the detection window in a history DataBase (DB). The information stored in the history DB comprises synchronization information obtained at the previous DRX occasions. For each DRX occasion, the history DB takes actions according to the result of the synchronization procedure. As the synchronization procedure is requested to detect a target SSB, the history DB conducts *APPLY HISTORY* if it finds appropriate history information that matches with the target SSB. When the synchronization procedure detects an SSB successfully, the history DB conducts *STORE HISTORY* and stores the result as history information. On the other hand, if the synchronization fails to detect the target SSB based on the history information, it conducts *REMOVE HISTORY* and removes the history information.

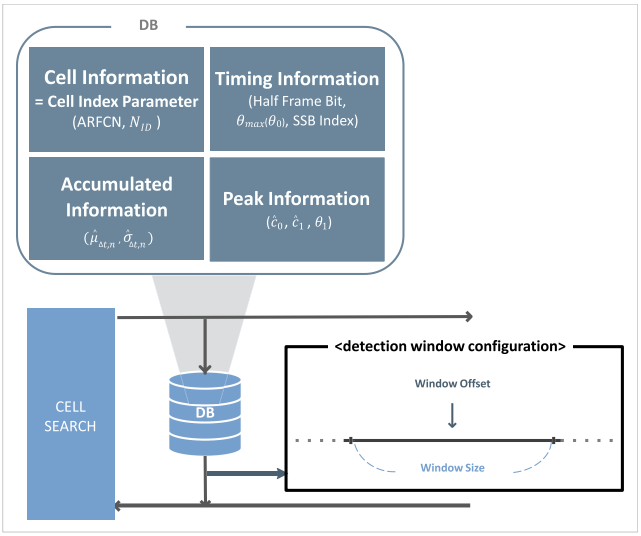

FIGURE 3. The overall structure of the history DB.

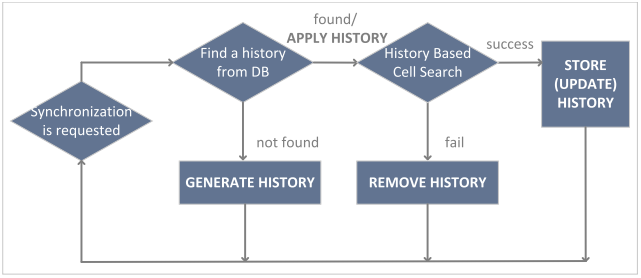

FIGURE 4. The operational flow in terms of the history DB.

Each history information contains various parameters described in Fig. 3 and derived from the previous synchronization procedures. The parameters are mainly categorized into *Cell Information*, *Timing Information*, *Accumulated Information*, and *Peak Information*. The Cell Information includes basic cell parameters such as center frequency and N_{ID}. The Timing Information corresponds to the timing offset, half frame bit, and SSB index obtained in the previous synchronization process. The Accumulated Information corresponds to the statistics of detected timing offsets during past DRX occasions. The Peak Information includes the correlation results of multiple paths. These parameters are essential to determine the detection window size by considering the drift and the multi-path of timing offset.

Fig. 4 depicts how the history DB works according to the synchronization process. If the synchronization process is successful, the history DB issues STORE HISTORY and stores the result as the history information. If there is no history information whose Cell Information does not match, the history DB issues *GENERATE HISTORY*, and the history information is newly generated. Otherwise, the history DB updates the Timing, Accumulated, and Peak Information of the existing history information whose Cell Information matches. On the other hand, if the synchronization process fails, the history DB issues REMOVE HISTORY, removing from the extant history information whose Cell Information matches from the history DB. This procedure leads the following synchronization process to try the PSS detection for the whole range of received samples.

Before a synchronization procedure, the history DB finds proper history information whose Cell Information matches with the target SSB. If all the parameters in the Cell Information match, then the detection window is configured for the current DRX occasion based on the history information and used for the PSS detection. The configuration determines the offset and size of the detection window and requires an algorithmic approach considering the characteristics of time-varying factors. The offset of the detection window should be configured according to how timing offset drifts over time due to sampling clock offset. The size of the detection window should be configured according to how randomly timing offset varies by channel.

B. DECIDING DETECTION WINDOW OFFSET AND SIZE BY VARIANCE ACCUMULATION

The proposed scheme configures the offset and size of the detection window based on the previous timing offset. Let $\theta_{max,n}$ denote the timing offset detected at the n-th DRX occasion. Since the sampling clock offset between the gNB and the UE is constant over time, the amount of the drift is basically proportional to the timing interval between two successive DRX occasions. Also, the timing offset may drift randomly due to the effect of time-varying channel. Therefore, we can consider $\theta_{max,n}$ in a mathematical model as follows,

$$\theta_{max,n} = \theta_{max,n-1} + W_n \tag{8}$$

where W_n is a Gaussian random variable whose mean and variance are $\mu_{\Delta\theta}$ and $\sigma^2_{\Delta\theta}$, respectively. Based on (8), the proposed scheme estimates $\mu_{\Delta\theta}$ by averaging the difference between the current and previous timing offsets. Let $\hat{\mu}_{\Delta\theta,n}$ denote the estimated $\mu_{\Delta\theta}$ at the n-th DRX occasion, then

$$\hat{\mu}_{\Delta\theta,n} = \frac{\sum_{k=2}^{n}(\theta_{max,k} - \theta_{max,k-1})}{n-1} \tag{9}$$

$$= \frac{(\theta_{max,n} - \theta_{max,n-1}) + (n-2)\hat{\mu}_{\Delta\theta,n-1}}{n-1}. \tag{10}$$

Since $\theta_{max,n-1}$ can be derived from the Timing Information of the corresponding history information, $\mu_{\Delta\theta,n}$ can be iteratively derived from $\theta_{max,n-1}$ at the n-th DRX occasion. As guided by (10), the proposed scheme calculates the difference between the current and previous timing offsets and accumulates it to the history information for every DRX occasion. The proposed scheme then configures the detection window offset as $\mu_{\Delta\theta,n}$ at the $(n+1)$-th DRX occasion.

The scheme configures the detection window size based on the estimated variance of W_n. The variance of W_n can be estimated from how the timing offsets previously detected differ from the estimated mean in a Mean Squared Error

(MSE) perspective. The MSE in n-th DRX occasion, denoted by $\hat{\sigma}^2_{\Delta\theta,n}$, can be derived as follows,

$$\hat{\sigma}^2_{\Delta\theta,n} = \frac{1}{n}\sum_{k=1}^{n}(\theta_{max,n} - \mu_{\Delta\theta,n})^2 \tag{11}$$

$$= \frac{1}{n}\left((\theta_{max,n} - \hat{\mu}_{\Delta\theta,n})^2 + (n-1)\hat{\sigma}^2_{\Delta t,n-1}\right). \tag{12}$$

For each DRX occasion, $\hat{\sigma}^2_{\Delta\theta,n}$ is stored in the Accumulated Information of the corresponding history information and utilized for deriving $\hat{\sigma}^2_{\Delta\theta,n+1}$ in the $(n+1)$-th DRX occasion.

The detection window size at the n-th DRX occasion can be properly decided based on $\hat{\sigma}^2_{\Delta\theta,n}$ and how precisely the proposed scheme aims to detect the PSS. The probability that the timing $\theta_{max,n}$ is in $\mathbf{R}_a = [\mu_{\Delta\theta,n} - a/2, \mu_{\Delta\theta,n} + a/2]$ calculated as follows,

$$P(\theta_{max,n} \in \mathbf{R}_a) = \int_{-a/2}^{a/2} \frac{1}{\sqrt{2\pi}\sigma_{\Delta\theta,n}} e^{-\frac{z^2}{2\sigma^2_{\Delta\theta,n}}} dz \tag{13}$$

$$= 2\left(1 - Q\left(\frac{a}{2\sigma_{\Delta\theta,n}}\right)\right). \tag{14}$$

If the proposed scheme aims to detect the PSS with the probability of $Pr_{detectPSS}$, then the detection window size at the n-th DRX occasion, denoted by a_n, is configured as follows,

$$a_n = 2\sigma_{\Delta\theta,n}Q^{-1}\left(1 - \frac{Pr_{detectPSS}}{2}\right). \tag{15}$$

Since $Q^{-1}\left(1 - \frac{Pr_{detectPSS}}{2}\right)$ is constant for n, the derivation of a_n is straightforward after $\sigma_{\Delta\theta,n}$ is calculated at the n-th DRX occasion.

C. SECOND PATH EXTENSION

The proposed scheme can reduce the computational complexity of the PSS detection by configuring a proper detection window as above. On the other hand, the configuration of a compact detection window may cause the proposed scheme to miss-detect the best timing offset in a multi-path channel environment. Fig. 5 shows the examples of PSS detection results where two considerable paths are detected. Although the left peak was the strongest at the previous DRX occasion, the right peak becomes stronger at the current DRX occasion. If the detection window is compactly configured and only includes the timing of the left peak, then the window will lead to miss-detecting the right peak.

Therefore, the detection window configuration needs to consider other multi-paths when they are expected to grow at the next DRX occasion. If the proposed scheme detects other paths that are received at a sufficiently strong level via the PSS correlation, it extends the detection window whose range includes the offsets of the paths. If we denote the offset of the j-th strongest path by θ_j so $\theta_0 = \theta_{max}$, the strength of each peak can be estimated by the amplitude of

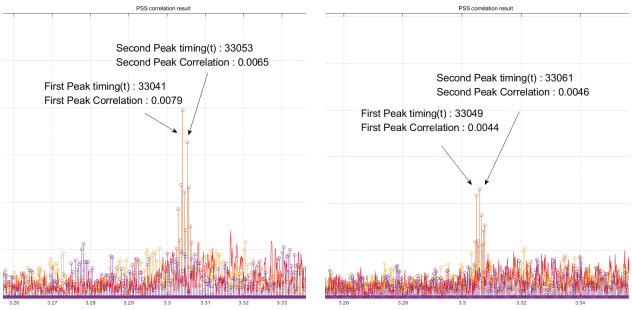

(a) (b)

FIGURE 5. Examples of PSS detection results in a commercial multi-path environment.

the correlation as follows,

$$\left|\rho_i[\theta_j]\right| = \left|\sum_{k=0}^{N-1} h[\theta_j + k] \cdot |p_i[k]|^2 + \sum_{k=0}^{N-1} z[\theta_j + k] \cdot p_i[k]\right| \tag{16}$$

$$\simeq P_{PSS}\left|\sum_{k=0}^{N-1} h[\theta_j + k]\right|, \tag{17}$$

where P_{PSS} denotes the power of the transmitted preamble signal and is constant for i and j. Since the amplitude of the channel impulse response is proportional to $|\rho_i[\theta_j]|$, the proposed scheme can regard $\left|\rho_i[\theta_j]\right|$ as the strength of the j-th path.

Based on the strength of the multiple paths, the proposed scheme decides whether to extend the detection window to θ_j. The detection window is extended if the probability that the j-th path gets stronger than the strongest path is sufficiently high. The probability can be derived from Rayleigh cumulative distribution function which is expressed as follows,

$$F(c_j|\sigma_j) = 1 - \exp(\frac{-c_j^2}{2\sigma_j^2}), \tag{18}$$

where c_j corresponds to the strength of the j-th path and is equivalent to $\rho_i^2[\theta_j]$, and σ_j is the Rayleigh scalar parameter for the j-th path.

(18) provides how the strength of the j-th path will be at the next DRX occasion and helps the proposed scheme decides whether to extend the detection window to θ_j or not. Fig. 6 illustrates the overall procedure of the proposed scheme. It initially checks criterion 1 and sees if the path at θ_0 was sufficiently strong for conducting the synchronization procedure at the previous DRX occasions. Otherwise, the proposed scheme checks criterion 2 and estimates whether the path at θ_1 is likely to become stronger than the path at θ_0. In this case, it needs to try synchronization with the path at

θ_1 as well as the one at θ_0. If the path at θ_1 is also weak, then the proposed scheme tries to detect all the paths nearby θ_0.

Let α_{sync} denote the minimal level of $\rho_i[\theta_j]$ that the synchronization procedure succeeds. (α_{sync} can be figured out as the minimal level of received signal strength that can achieve the target block error rate of the PBCH by the rule of thumb.) If the history information includes the average of c_0, denoted by $\hat{c_0}$, the proposed scheme checks whether $\hat{c_0} < \alpha_{sync}$. If the criterion holds, then the detection window is extended for considering the other paths. On the other hand, if the criterion does not hold, the window is configured as in case 1 of Fig. 6.

The extension of the detection window happens in two ways based on the strength of the second path. If the proposed scheme estimates that the path at c_1 may get stronger than the first path, the proposed scheme compactly extends the detection window to include θ_1. Otherwise, the proposed scheme extends the detection window size to the length of a CP. If we approximate that $\sigma_0^2 \simeq \sigma_1^2$ when c_1 gets similar with c_0, the probability that c_1 exceeds c_0 at the next DRX occasion will be derived as follows,

$$P(c_0 \leq c_1) = 1 - \exp(\frac{-\hat{c_1}^2}{2\sigma_0^2}). \tag{19}$$

With $\hat{c}_0$ provided by the history information, we can consider that

$$\hat{c}_1 = \beta_n; \hat{c}_0 = \beta_n(\sigma_0\sqrt{\frac{\pi}{2}}), \tag{20}$$

where β_n denotes the ratio of $\hat{c_1}$ and $\hat{c_0}$ observed at the n-th DRX occasion. Substituting (20), (19) is further simplified as follows,

$$\begin{aligned} P(c_0 \leq c_1) &= 1 - \exp(\frac{-\hat{c_1}^2}{2\sigma_0^2}) \qquad (21)\\ &= 1 - \exp(-\frac{\beta_n^2 \cdot \sigma_0^2 \cdot (\pi/2)}{2\sigma_0^2})\\ &= 1 - \exp(\frac{\pi}{4}\beta_n^2). \qquad (22) \end{aligned}$$

(22) enables to derive the probability that c_1 gets stronger than c_0 at the next DRX occasion based on β_n. Table. 1 shows the relationship between β_n and the probability. Let us denote the minimum probability that c_1 gets larger than c_0 by γ. The proposed scheme configures the window as in case 2 if $P(c_0 \leq c_1) > r$, otherwise configures it as in case 3. Then, the threshold of β_n for the criterion 2, denoted by β_{sync}, is derived as follows,

$$\beta_{sync} = \sqrt{\frac{\ln(1-\gamma)}{\frac{\pi}{4}}}. \tag{23}$$

The proposed scheme can determine whether to extend the detection window to θ_1 if β_n is larger than β_{sync}.

IV. PERFORMANCE EVALUATION

For over-the-air verification, we build and experiment with a Software Defined Radio (SDR) testbed which proceeds

TABLE 1. Relationship between β_n and $P(c_0 \leq c_1)$.

β_n[dB]	$P(c_0 \leq c_1)$
-1	0.390765934
-2	0.268510667
-3	0.179041812
-4	0.117041625
-5	0.07553475
-6	0.048347445
-7	0.030783498
-8	0.01953498
-9	0.01237057
-10	0.00782322

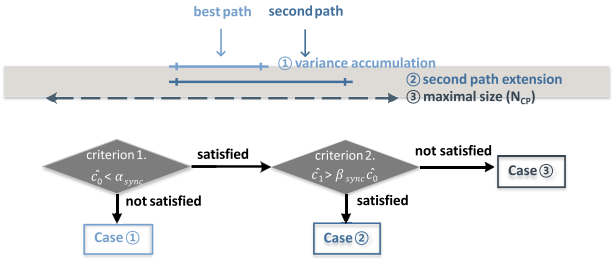

FIGURE 6. The procedure for configuring the detection window.

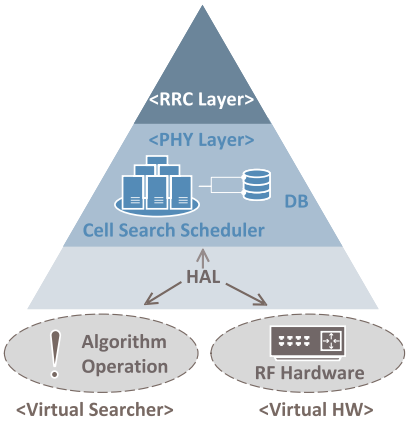

FIGURE 7. SW architecture of the implemented UE.

synchronization in real time. The testbed consists of emulated gNB and UE which play roles of signal transmission and reception, respectively. Each of the gNB and UE has a Universal Software Radio Peripheral (USRP) B210 which generates or samples RF signal [31]. We utilize Open Air Interface (OAI) software to generate the baseband signal of the gNB [32]. For baseband signal processing at the UE, we employ the cell search software whose architecture is described in Fig. 7 [33]. The proposed scheme is implemented in the PHY layer of the UE software.

Experiments are conducted via laboratory and field tests as illustrated in Fig. 8. During the laboratory test, the signal emitted from the USRP of the gNB passes through conduction cables and suffers fading channel emulated by a Spirent Vertex Channel Emulator. The center frequency of the USRPs

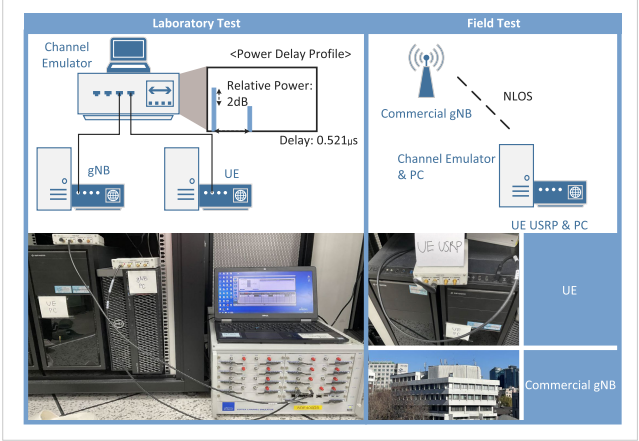

FIGURE 8. The test environments of the laboratory and field tests.

TABLE 2. Frame parameters.

Parameters	laboratory	field
ARFCN	-	643488
Downlink Frequency	3300MHz	3452.32MHz
Subcarrier Spacing(Δf))	30kHz	
Numerology(μ)	1	
FFT size(N_{FFT})	1024	
Cell ID	923(NID1:307, NID2:2)	
SSB index	2,3,4	
N_{CP}	72	
$\lvert\theta_1 - \theta_0\rvert$	20	
β_n	-2dB	
CFO	600 – 800Hz	
sampling error	50.78 samples/1 sec	

is set to 3.3GHz so that the experiments are not affected by signals from commercial gNBs and UEs. In the field test, the USRP of the UE receives via a 3.5GHz antenna and samples signal emitted from a nearby commercial SK Telecom gNB. The other frame parameters of both tests are configured as in Table 2. We configure the channel emulator to simulate the wireless channel experienced in the field test so that the channels of the two tests are equivalent. Also, CFO and sampling error are measured as in Table 2.

Through the tests, we measure Block Error Rate (BLER) and computational complexity for various schemes. The BLER is measured as the ratio of the number of PBCH decoding failures to the total number of trials. The conventional scheme with wide search detects the PSS within a fixed window whose size is $2N_{CP} = 144$. The conventional scheme with narrow search detects the PSS within a fixed window whose size is 16. The proposed scheme with variance accumulation configures the window size based on the variance accumulation and does not consider the second path at θ_1. The proposed scheme with second path extension configures the detection window size based on the accumulated variance and the second path at θ_1. For the proposed scheme with second peak extension, we decide α_{sync} and β_{sync} based on repeated experiments. α_{sync} is decided as the minimal $\rho_i[\theta_0]$ that enables the synchronization procedure to succeed with

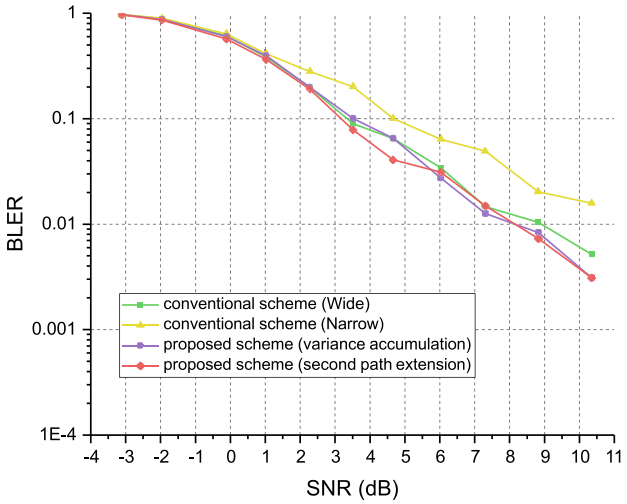

FIGURE 9. BLER performance in the laboratory test.

the probability of 90%. β_{sync} is considered as -4dB so that the window is extended to θ_1 if $\gamma = 0.1$.

A. SYNCHRONIZATION FAILURE PROBABILITY

Fig. 9 shows the BLER performance in the case of the laboratory test. (Fig. 9 does not provide the results when the SNR is higher than 10dB, because the BLER drastically decreases in that SNR range.) The results prove the necessity of the detection window adaptation since the conventional scheme with narrow search tends to fail synchronization more than the other schemes. Based on the criterion of 10% probability, the detection window adaptation can achieve the SNR gain by 1dB. The results also show that the proposed schemes perform similarly to the conventional scheme with wide search. This implies that the proposed scheme properly adapts the detection window based on history information. In addition, we can see that the proposed scheme with second path extension is effective when the SNR is 3.5–6dB. This is because the detection window is only extended when the strength of the strongest path is below the threshold, and there are no valid paths in synchronization when the SNR is less than a certain level. Taking into account the systematic test environment, we can consider the performance gain by the proposed scheme as a sufficient level. Therefore, we can conclude that the proposed scheme with second path extension properly adapts the detection window according to the multi-path channel environment and without any side effects.

Fig. 10 summarizes the BLER results of the field test when the SNR is between 0–7dB. Except for the conventional scheme with narrow search, the results are similar to the ones in the laboratory test. (The result of the conventional scheme with narrow search gets better since the timing offset drift for the commercial gNB is more stable.) The proposed scheme with variance accumulation performs well and similar with the conventional scheme with wide search, and the second path extension improves synchronization performance.

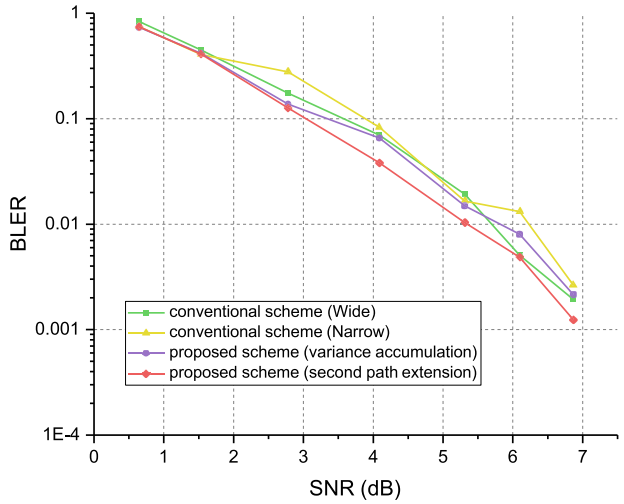

FIGURE 10. BLER performance in the field test.

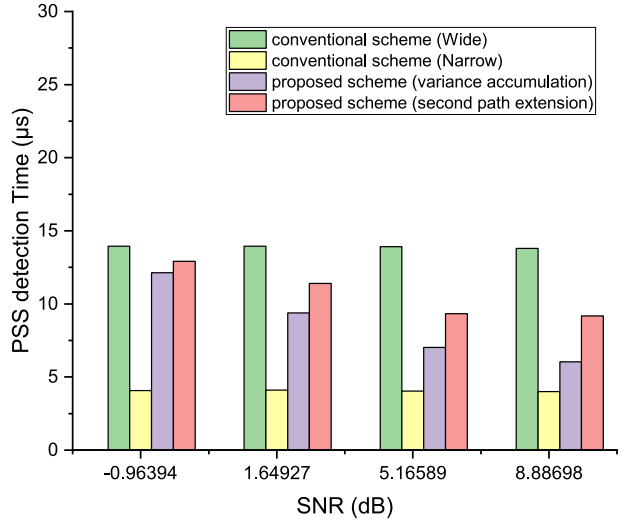

FIGURE 11. Average measured time of the PSS detection.

Therefore, the results prove that the advantages of the proposed scheme shown in the laboratory test are practically valid in commercial environments.

B. COMPUTATIONAL COMPLEXITY

Fig. 11 shows the average measured time of the PSS detection during the laboratory test. Configuration of the detection window is essential for synchronization at DRX occasions since the PSS detection based on any detection window takes less than 15 us meanwhile the PSS detection for the whole range takes 45930.63 us. Compared with the conventional schemes, the proposed scheme additionally reduces the time by managing the detection window more compactly when the SNR is 3.5–10dB. The proposed scheme with variance accumulation and second peak extension reduces the time by 6.537us (52.81%) and 9.258us (33.17%), respectively. The results also show that the proposed scheme with second path extension can properly take additional computational complexity in trade-off to enhance the synchronization performance by extending the detection window compared to variance accumulation.

V. CONCLUSION

It is essential for the 5G UEs in an RRC_IDLE state to achieve synchronization in a short time for each DRX occasion. To do so, we propose an efficient PSS detection scheme that configures the detection window based on the history information. The proposed scheme utilizes the statistics of timing offset previously detected for deciding the detection window. The proposed scheme also extends the detection window adaptively for handling multiple paths so that further synchronization is more likely to succeed. The experimental results prove that the proposed scheme can effectively reduce the computational complexity of overall synchronization and enhance synchronization performance.

The proposed scheme in this paper contributes to the reduction of computational burden during the wake-up procedure in DRX occasions. Managing the detection window based on a multi-path environment ultimately realizes low-power and short-delay communications in 5G. Also, the experimental results are notable since they prove the enhancement of BLER performance in practical channel environments. To demonstrate how the proposed scheme can be extensively applied, further studies should be investigated in various channel and moving scenarios.

REFERENCES

[1] M. K. Maheshwari, M. Agiwal, and A. R. Masud, "Analytical modeling for signaling-based DRX in 5G communication," *Trans. Emerg. Telecommun. Technol.*, vol. 32, no. 1, p. e4125, Jan. 2021.

[2] C. S. Bontu and E. Illidge, "DRX mechanism for power saving in LTE," *IEEE Commun. Mag.*, vol. 47, no. 6, pp. 48–55, Jun. 2009.

[3] A. Agiwal and M. Agiwal, "Enhanced paging monitoring for 5G and beyond 5G networks," *IEEE Access*, vol. 10, pp. 27197–27210, 2022.

[4] D. B. Dash, G. Ponnamreddy, U. C. Baskar, and D. P. Basavaraj, "Adaptive DRX mechanism to improve energy effciency and to reduce page delay for VoWiFi devices," in *Proc. IEEE Women Technol. Conf. (WINTECHCON)*, Jun. 2022, pp. 1–5.

[5] A. K. Sultania, C. Delgado, and J. Famaey, "Implementation of NB-IoT power saving schemes in ns-3," in *Proc. Workshop Next-Gener. Wireless NS-3*, Jun. 2019, pp. 5–8.

[6] N. Saxena, A. Roy, M. K. Maheswari, E. Rastogi, and D. R. Shin, "DRX in new radio unlicensed: A step beyond 5G wireless," *IEEE Commun. Mag.*, vol. 59, no. 1, pp. 82–88, Jan. 2021.

[7] M. Agiwal and H. Jin, "Directional paging for 5G communications based on partitioned user ID," *Sensors*, vol. 18, no. 6, p. 1845, Jun. 2018.

[8] C. Hu and Y. Zhang, "5G NR primary synchronization signal detection with low hardware resource occupancy," in *Proc. IEEE/CIC Int. Conf. Commun. China (ICCC)*, Aug. 2018, pp. 304–308.

[9] Y.-H. You and H.-K. Song, "Efficient sequential detection of carrier frequency offset and primary synchronization signal for 5G NR systems," *IEEE Trans. Veh. Technol.*, vol. 69, no. 8, pp. 9212–9216, Aug. 2020.

[10] M. H. Nassralla, M. M. Mansour, and L. M. A. Jalloul, "A low-complexity detection algorithm for the primary synchronization signal in LTE," *IEEE Trans. Veh. Technol.*, vol. 65, no. 10, pp. 8751–8757, Oct. 2016.

[11] Z. Zhang, M. Lei, K. Long, and Y. Fan, "Improved cell search and initial synchronization using PSS in LTE," in *Proc. IEEE 75th Veh. Technol. Conf. (VTC Spring)*, May 2012, pp. 1–5.

[12] D. Wang, Z. Mei, H. Zhang, and H. Li, "A novel PSS timing synchronization algorithm for cell search in 5G NR system," *IEEE Access*, vol. 9, pp. 5870–5880, 2021.
[13] M. Morelli and M. Moretti, "A robust maximum likelihood scheme for PSS detection and integer frequency offset recovery in LTE systems," *IEEE Trans. Wireless Commun.*, vol. 15, no. 2, pp. 1353–1363, Feb. 2016.
[14] M. Morelli, G. Imbarlina, and M. Moretti, "Estimation of residual carrier and sampling frequency offsets in OFDM-SDMA uplink transmissions," *IEEE Trans. Wireless Commun.*, vol. 9, no. 2, pp. 734–744, Feb. 2010.
[15] M. Morelli and M. Moretti, "Fine carrier and sampling frequency synchronization in OFDM systems," *IEEE Trans. Wireless Commun.*, vol. 9, no. 4, pp. 1514–1524, Apr. 2010.
[16] F. Wen, J. Kulmer, K. Witrisal, and H. Wymeersch, "5G positioning and mapping with diffuse multipath," *IEEE Trans. Wireless Commun.*, vol. 20, no. 2, pp. 1164–1174, Feb. 2021.
[17] M. Usman Hadi, T. Jacobsen, R. Abreu, and T. Kolding, "5G time synchronization: Performance analysis and enhancements for multipath scenarios," in *Proc. IEEE Latin-Amer. Conf. Commun. (LATINCOM)*, Nov. 2021, pp. 1–5.
[18] C. E. O'Lone, H. S. Dhillon, and R. M. Buehrer, "Characterizing the first-arriving multipath component in 5G millimeter wave networks: TOA, AOA, and non-line-of-sight bias," *IEEE Trans. Wireless Commun.*, vol. 21, no. 3, pp. 1602–1620, Mar. 2022.
[19] Y. Tsuchida, S. Nagata, and M. Sawahashi, "Cell search time performance using multipath signals in LTE downlink," in *Proc. IEEE 73rd Veh. Technol. Conf. (VTC Spring)*, May 2011, pp. 1–5.
[20] J. Liu, K. Mei, X. Zhang, D. McLernon, D. Ma, J. Wei, and S. A. R. Zaidi, "Fine timing and frequency synchronization for MIMO-OFDM: An extreme learning approach," *IEEE Trans. Cognit. Commun. Netw.*, vol. 8, no. 2, pp. 720–732, Jun. 2022.
[21] S. K. Vankayala, J. Akhtar, K. S. A. Krishnan, and A. K. Sah, "Accelerated detection schemes for PSS in 5G-NR," in *Proc. IEEE 3rd 5G World Forum (5GWF)*, Sep. 2020, pp. 460–466.
[22] C. Qing, S. Tang, X. Cai, and J. Wang, "Lightweight 1-D CNN-based timing synchronization for OFDM systems with CIR uncertainty," *IEEE Wireless Commun. Lett.*, vol. 11, no. 11, pp. 2375–2379, Nov. 2022.
[23] X. Yang, Y. Xiong, G. Jia, W. Fang, and X. Zheng, "PSS based time synchronization for 3GPP LTE downlink receivers," in *Proc. IEEE 13th Int. Conf. Commun. Technol.*, Sep. 2011, pp. 930–933.
[24] M. R. Sriharsha, S. Dama, and K. Kuchi, "A complete cell search and synchronization in LTE," *EURASIP J. Wireless Commun. Netw.*, vol. 2017, no. 1, pp. 1–14, Dec. 2017.
[25] A. A. D'Amico, M. Morelli, and M. Moretti, "A novel scheme for CP-length detection and initial synchronization for the LTE downlink," *IEEE Trans. Wireless Commun.*, vol. 18, no. 10, pp. 4668–4678, Oct. 2019.
[26] *NR; User Equipment (UE) Procedures in Idle Mode and in RRC Inactive State*, document G. T. 38.304, 2022.
[27] *NR; Medium Access Control (MAC) Protocol Specification*, document G. T. 38.321, 2021.
[28] *NR; Radio Resource Control (RRC); Protocol Specification*, document G. T. 38.331, 2022.
[29] *NR; Medium Access Control (MAC) Protocol Specification*, document G. T. 38.213, 2021.
[30] *NR; Physical Channels and Modulation*, document G. T. 38.211, 2022.
[31] Ettus Research. *USRP B210 USB Software Defined Radio (SDR)*. Accessed: Dec. 20, 2022. [Online]. Available: https://www.ettus.com/all-products/ub210-kit/
[32] *5G Software Alliance for Democratising Wireless Innovation*. Accessed: Dec. 20, 2022. [Online]. Available: https://openairinterface.org/
[33] J. Y. Han, O. Jo, and J. Kim, "Exploitation of channel-learning for enhancing 5G blind beam index detection," *IEEE Trans. Veh. Technol.*, vol. 71, no. 3, pp. 2925–2938, Mar. 2022.

SUBIN JEONG (Student Member, IEEE) is currently pursuing the B.S. degree with the Department of Electronics Engineering, Sookmyung Women's University, Seoul, South Korea.

JUYEOP KIM (Member, IEEE) received the B.S. and Ph.D. degrees in electrical engineering from the Korea Advanced Institute of Science and Technology (KAIST), in 2004 and 2010, respectively. He is currently an Assistant Professor with the Department of Electronics Engineering, Sookmyung Women's University, Seoul, South Korea. His current research interests include softwarized modems and next-generation wireless communication.